J. Synchrotron Rad. (1999). **6**, 688–690

X-ray magnetic circular dichroism used to image magnetic domains

Peter Fischer,[a]* Thomas Eimüller,[a] Regina Kalchgruber,[a] Gisela Schütz,[a] Günter Schmahl,[b] Peter Guttmann[b] and Günther Bayreuther[c]

[a]Univ. Würzburg, Exp. Physik IV, Am Hubland, D 97074 Würzburg Germany, [b]Univ. Göttingen, FE Röntgenphysik, Geiststr. 11 D 37073 Göttingen Germany, and [c]Univ. Regensburg, Inst. f. Exp. u. Angew. Physik, D 93040 Regensburg Germany. E-mail: peter.fischer@physik.uni-wuerzburg.de

A new technique to image magnetic domain structures has been established by the combination of the high resolution transmission X-ray microscope (TXM) at BESSY I based on the zone plate technique with the X-ray magnetic circular dichroism (X-MCD) providing a huge magnetic contrast. A lateral spatial resolution down to 30 nm could be achieved. Basic features of X-MCD are the inherent element-specificity and the potential to gain information on the local spin and orbital moments of the absorbing species applying magneto-optical sum rules. Key results at the Fe $L_{3,2}$ edges of Fe in a layered GdFe system and at the Co L_3 edge of a PtCo layered system demonstrate the potential of this microscopy. The images can be recorded in varying magnetic fields which allows to study the evolution of magnetic domains within a complete hysteresis loop.

Keywords: magnetic domain imaging; transmission X-ray microscopy; X-ray magnetic circular dichroism.

1. Introduction

The imaging of magnetic microstructures is an outstanding challenge both in current research of magnetism and its technological applications. Progress in the understanding of phenomena like the occurence of the GMR, quantum oscillations or the magnetic interface anisotropy benefits from recent technical developments to visualize magnetic domains. Important issues as e.g. the exploration of the limitations of future technical magnetic devices like the bit size in high density recording systems or the exact switching behaviour of magnetic dots in nanostructured systems on a typical length scale of 1-100 nm and a quantitative information on the local magnetization scanned over areas with dimensions extending to several μm as a function of applied magnetic fields can be addressed. Powerful magnetic imaging techniques with high spatial resolution have thus been developped. However, methods based on electron detection, like SEMPA, SPLEEM are restricted to zero field studies, while techniques detecting the stray field of the magnetic sample like MFM or Lorentz microscopy provide only an indirect information on the local magnetization. On the other hand the established Kerr-microscopy which detects photons is diffraction limited by the wave length of visible light.

The effect of X-ray magnetic circular dichroism (X-MCD), which is the X-ray counterpart to the magneto-optical Kerr-effect (MOKE) occurs in the vicinity of element-specific inner-core absorption edges. It can be defined as the dependence of the absorption of circular polarized X-rays on the projection of the magnetization onto the photon propagation direction in ferromagnetic samples. At L-edges in $3d$ transition metals relative changes in the absorption cross section up to 50% occur, so that X-MCD can serve as a huge magnetic contrast in imaging techniques which are based on photon absorption. The first attempt using X-MCD in magnetic microscopy involved a photoemission microscope (PEEM) (Stoehr et al., 1993) where a spatial resolution of a few μm could be obtained. This experiment, however, is restricted to studies in zero magnetic field. Several attempts are currently on the way to use X-MCD for the imaging of magnetic domains, see e.g. Warwick et al., 1998. A new concept to image magnetic domains even on the nm scale is the combination of a high resolution transmission X-ray microscope (TXM) with X-MCD in the complementary transmission mode (Magnetic TXM = M-TXM) (Fischer et al., 1996).

2. Magnetic contrast with X-MCD

In the absorption process of circularly polarized X-rays at spin-orbit split L-edges the photoelectron is excited from an inner-core p-level into an unoccupied state with d-symmetry above the Fermi level. Due to spin-orbit interaction in the initial state, angular momentum conservation and the constraint that $\Delta m_l = \pm 1$ it acquires both an expectation value of the spin $< \sigma_z >$ and the orbital $< l_z >$ momentum projected onto the photon propagation direction. This polarized photoelectron can therefore be considered as a local probe for the spin and orbital polarization of the final states in the absorbing atom according to the principle of Pauli. In the atomic case the polarization of the photoelectron can be determined taking into account Clebsch-Gordan coefficients and transition probabilities and amounts to $< \sigma_z >= -50\%$ and $+25\%$ at the L_2 and L_3 edges, while $< l_z >= +75\%$ at both $L_{2,3}$ edges. As the absorption coefficient can be described within Fermi's golden rule the exchange interaction in a spin ferromagnet shifting spin-up and spin-down bands is responsible for the polarization dependence of the transition probability in the absorption process. Thus the magnetization of the absorbing atom is reflected by the absorption coefficients with the direction of the magnetization parallel μ^+ and antiparallel μ^- to the photon propagation direction. In the case of an ideal ferromagnet the dichroic signal, i.e. the difference $(\mu^+ - \mu^-)$ normalized to the unpolarized absorption $(\mu^+ + \mu^-)$ corresponds directly to $< \sigma_z >$ provided that the corresponding orbital polarization can be neglected. Otherwise the dichroic signal would increase/decrease at the L_3/L_2 edge, respectively.

Therefore the huge magnetic contrast that can be used in imaging techniques relying on X-MCD in the transmission mode is provided by the energy-dependent, element-selective and symmetry-sensitive deviation of the absorption coefficient $\Delta\mu(E)$ relative to the polarization averaged absorption coefficient $\mu_{|i>}(E)$ which takes into account only the photoprocess in an atomic corel level $|i>$

$$\frac{\Delta\mu}{\mu_{|i>}}(E) = \frac{\sigma_c}{\sigma_{|i>}}(E)(\hat{m}\cdot\hat{e}_z)P_c. \qquad (1)$$

Thereby $(\hat{m}\cdot\hat{e}_z)$ denotes the projection of the normalized magnetic moment $\hat{m} = \frac{\vec{m}}{|\vec{m}|}$ onto the propagation direction with unit vector $\hat{e}_z$ of the photons with a degree of circular polarization P_c. The value of $\mu_{|i>}(E)$ is specific and can be taken from spectroscopic data tables. The value of $\Delta\mu$ reflecting the contrast, however, has to take into account background extinction due to absorption in higher levels. This contribution is larger e.g. at the Fe L_2 edge than at the corresponding L_3 edge, yielding a weaker contrast at the former edge. However, this is partly compensated due to the higher value of $< \sigma_z >$ at the L_2 edge. As the magnetic absorption cross section normalized to the polarization averaged atomic cross section

$\frac{\sigma_c}{\sigma_{|i>}}$ can be determined by e.g. X-MCD studies it can be seen from eq. (??) that provided P_c is known the observable experimental quantity ($\Delta\mu(E)$) allows a quantitative determination of the absolute magnetic moment projection of the absorbing atom. Even more important, however, is the virtue of X-MCD to extract separately the spin and the orbital moments by applying the sum-rules to corresponding data at spin-orbit split initial states (Thole et al., 1992 and Carra et al., 1993). Thus the orbital moment, which plays an important role in magnetism as e.g. the origin of the magnetocrystalline anisotropy energy in thin films has attracted growing interest recently.

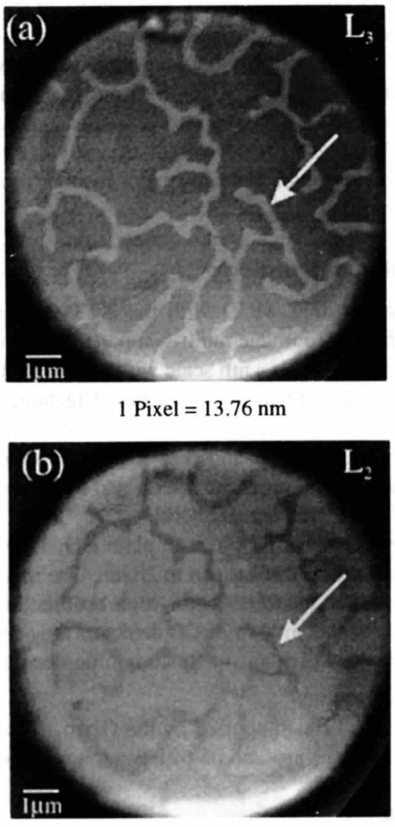

Figure 1
Magnetic images of a sputtered multilayered 4ÅGd4Å Fe system taken at the Fe L_3 (a) and L_2 (b) edge (Fischer et al., 1998)

3. Experimental details

The X-ray optical set-up of the TXM, which is described in more detail in (Niemann et al., 1995 and Schmahl et al., 1995) is based on the zone plate technology. A condensor zone plate (CZP) ($D = 9mm$), which images the X-ray source into the object plane and an object field limiting pinhole ($d \approx 10 - 20\mu m$) act as linear monochromator due to the wave length dependence of the focal length of the CZP. The slight change in magnification according to the lense equation in optics is compensated by an adjustment of the position of the CCD camera. Thus the photon energy can be tuned to a value where the dichroic effect is maximum. The monochromaticity given by $\lambda/\Delta\lambda = D/2d = 225$ is sufficient to separate in particular the L_3 and the L_2 edges of Fe (Co) being separated by 13(15) eV. A microzone plate (MZP) with a spatial resolution of about $30nm$ generates a magnified image of the object, which is recorded with a slow scan CCD camera. This value of lateral resolution is determined from the observation of structures of such dimensions and is in agreement with the nominal resolution that could be estimated from the quality of the micro zone plate used.

In order to image magnetic domains slight modifications have been applied (Fischer et al., 1997). Circularly polarized light can be selected by partly masking the synchrotron beam ($P_c \approx 60\%$) and magnetic fields ($< 80mT$) can be provided to the sample by a solenoid with its field direction pointing parallel/antiparallel to the photon beam propagation direction.

The multilayered GdFe (75 × (4Å Gd/4Å Fe)) and PtCo (30 × (4.2Å Co/6.8Å Pt)+1005.8Å Pt) systems, which had been prepared by magnetron sputtering onto 325 nm thin polyimid substrates exhibited a strong anisotropy perpendicular to the surface, which was verified by MOKE magnetometry. Due to the low penetration depth of soft X-rays the use of thin substrates is crucial. However, this problem occurs similarly in transmission electron microscopy measurements and these two techniques can thus benefit from each other.

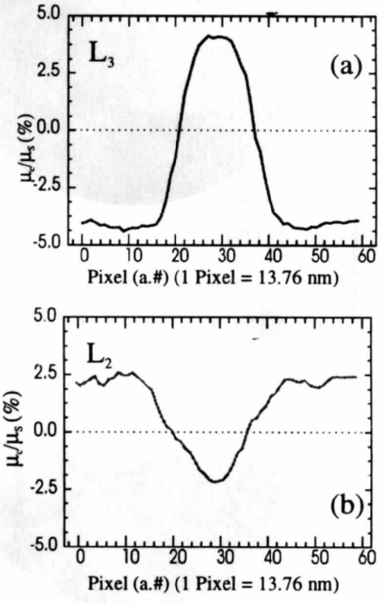

Figure 2
Corresponding scan profile across the domain indicated by the arrows (a,b) (Fischer et al., 1998)

4. Results and discussions

The potential and the characteristic feature of the M-TXM technique can be demonstrated by the following key results.

4.1. Magnetic images at Fe $L_{3,2}$ edges in a GdFe system

Figure 1 shows the magnetic X-ray microscopic images of the Gd/Fe system at the Fe L_3- (a) and L_2-edge (b) (Fischer et al., 1998). The dark/light areas in fig. 1 (a) indicate the direction of the local Fe magnetization projection in/out of the paper plane. The pattern at the L_2 edge (b) is inversed as expected from the different value of $< \sigma_z >$. Also the magnetic contrast is weaker at the L_2 edge by a factor of 2. This can be traced back to the signal-to-background ratio mentioned above. To quantify the contrast observed in the images a normalization to reference images with fully saturated magnetization (μ_c/μ_S) has been performed. Corresponding scan profiles (fig. 2 (a,b)), taken from a selected domain region

(see arrow in fig. 1 (a,b)) indicate that within the magnetic domain the full bulk-like Fe moment of $2.1\mu_B$ is established as expected from the MOKE measurements. This is also in accordance with eq.(??) as $(\hat{m} \cdot \hat{e}_z)$ is directly related to $\Delta\mu$ and the other quantities $\mu_{|i>}(E)$, $\frac{\sigma_c}{\sigma_{|i>}}(E)$ and P_c are known. Valuable information can be obtained regarding the observed width of the domain wall (fig. 2 (a,b)), which is related to fundamental anisotropy (K_u) and exchange constants (A) by $w \sim \sqrt{A/K_u}$. However, as w is expected to be of the order of $20nm$, this is below the present spatial resolution limit in our images.

4.2. Images at the Co L_3 edge of a PtCo system

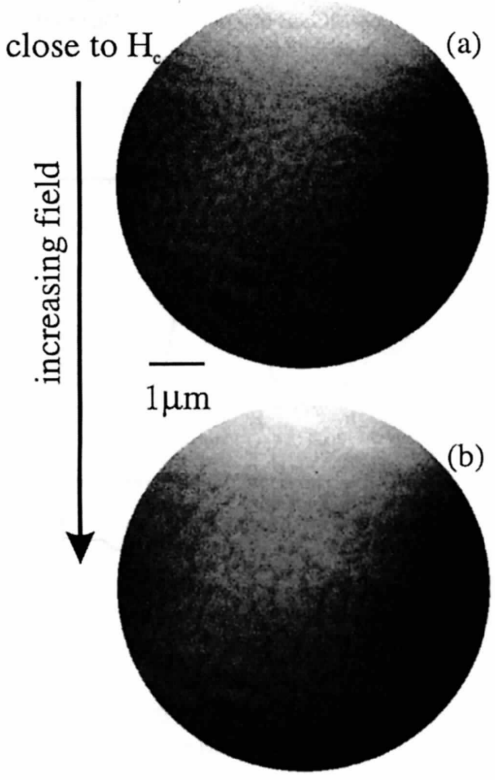

Figure 3
Magnetic images of a multilayered PtCo system taken at the Co L_3 edge close to the coercive field H_c (a) and at an increased field (b).

Another feature of high practical importance is the capability to take images in arbitrary applied magnetic fields, which allows to study the magnetization reversal process on a nanometer scale within a complete hysteresis cycle. A sampling of 75 images taken at the Fe L_3 edge in the multilayered GdFe system can be found under *http://www.physik.uni-augsburg.de/~fischer/gf6p-m3-en.mpg*. Another example demonstrating additionally the element-specificity is shown in fig. 3 where magnetic X-ray images obtained at the Co L_3 edge in the multilayered PtCo system are presented with the applied magnetic field varied between a value close to H_c (a) and an increased field (b). The magnetic contrast is much weaker compared to the Fe edges found in the GdFe system. Again this can be attributed to the signal-to-background ratio, which in the case of PtCo is dominated by the high Pt background contributing almost 95% to the absorption. The observed magnetic domain structures, which due to the element-specificity of the X-MCD correspond to the Co magnetization, exhibit a completely different shape compared to the GdFe system. Nucleation occurs very abruptly within a few Oe. Unfortunately the size of the observed fine structured irregular pattern is close to the resolution limit. At a moderate applied field (fig. 3 (a)) thin, worm-like domains with lengths of less than $1\mu m$ are observed. Their evolution with magnetic field is demonstrated in fig. 3 (b) where a stronger field $\approx 60mT$ is applied. The density of the thin domains has decreased, the shape of the remaining domains, however, has not changed, which indicates that here a nucleation dominated scenario is observed in contrast to the wall-moving scenario observed in the GdFe system. Up to now a quantitative analysis of the PtCo data accumulated so far is not possible mainly due to beam instabilites and the asymmetric arrangement leading to an inhomogeneous illumination of the sample.

5. Conclusion and outlook

The combination of X-MCD with the XTM is a new element-selective technique to image multi-component magnetic structures of technical relevance on a nm scale with a huge contrast. The particular feature inherent to all MCD based techniques to acquire information on the orbital moment via combined images taken at spin-orbit split initial states and applying the sumrules will be crucial for the understanding of the micro- and macroscopic magnetic properties of any ferromagnetic solid.

Future developments in the zone plate technique will improve the lateral spatial resolution down to 20 nm. The image acquisition rate will increase at next generation high brilliant SR-sources and current developments in X-ray CCD detectors thus approaching the μs read-out range which allows to study time-dependent effects.

Acknowledgements

This work has been supported by the German Federal Minister of Research (BMBF) proj. no.05 621 WAA and 05 644 WGA.

References

Stoehr, J., Wu, Y. Hermsmeier, B.D., Samant, M.G., Harp, G.R., Koranda, S. Dunham, D., & Tonner, B.T. (1993). *Science* **259**, 658–661.

Warwick, T., Anders, S., Hussain, Z., Lamble, G.M., Lorusso, G.F., MacDowell, A.A., Martin, M.C., McHugo, S.A., McKinney, W.R., & Pardmore, H.A., (1998), *Synchrotron Rad. News.*, **11(4)**, 5–22

Fischer, P., Schütz, G., Schmahl, G., Guttmann, P. & Raasch, D. (1996). *Z. Phys. B* **101**, 313–316.

Thole, B.T., Carra, P., Sette, F., & van der Laan, G. (1992). *Phys. Rev. Lett.* **68(12)**, 1943–1945.

Carra, P., Thole, B.T., Altarelli, M., & Wang, X. (1993). *Phys. Rev. Lett.* **70(5)**, 694–697.

Niemann, B., Schneider, G., Guttmann, P., Rudolph, D. & Schmahl, G. (1995), in *X-ray Microscopy IV* (V.V. Aristov and A.I. Erko eds) (Begorodski Pechatnik Publishing Company, Moscow), 66–75.

Schmahl, G., Rudolph, D., Guttmann, P., Schneider, G., Thieme, J. & Niemann, B. (1995). *Rev. Sci. Instrum.Journal* **66**, 1282–1286.

Fischer, P., Eimüller, T., Schütz, G., Guttmann, P., Schmahl, G., Pruegl, K. & Bayreuther, G., (1998) *J. Phys. D: Appl. Phys.* **31**, 649-655.

(Received 10 August 1998; accepted 3 December 1998)